NASA-TM-106694
19950019657

NASA Technical Memorandum 106694
ICOMP–94–16; CMOTT–94–4

Numerical Calculations of Shock-Wave/ Boundary-Layer Flow Interactions

P.G. Huang
Eloret Institute
Palo Alto, California

and

W.W. Liou
Institute for Computational Mechanics in Propulsion
and Center for Modeling of Turbulence and Transition
Lewis Research Center
Cleveland, Ohio

Prepared for the
First International Conference on Flow Interactions
sponsored by Hong Kong University
Hong Kong, September 5–9, 1994

National Aeronautics and
Space Administration

Numerical Calculations of Shock-Wave/Boundary-Layer Flow Interactions

P. G. Huang
Eloret Institute, Palo Alto, CA
Mailing Address:NASA Ames Research Center, Moffett Field, CA 94035
and
W. W. Liou
Center for Modeling of Turbulence and Transition
ICOMP, NASA Lewis Research Center, Cleveland, OH 44135

Abstract

The paper presents results of calculations for 2-D supersonic turbulent compression corner flows. The results seem to indicate that the newer, improved $k-\epsilon$ models offer limited advantages over the standard $k-\epsilon$ model in predicting the shock-wave/boundary-layer flows in the 2-D compression corner over a wide range of corner angles and flow conditions.

Introduction

Calculations of flows with shock-wave/boundary-layer interactions have become a major challenge in CFD in recent years. However, despite the significant advances in computational techniques in the past two decades, the ability of CFD in predicting the complexity of the flow field in regions of shock-wave/boundary-layer interactions may still hinge upon the choice of turbulence models. In most aerodynamic flow applications, zero-equation models have been used but there has been a shift to more complex field-equation type models in the last 5 years. The present paper reports the results of an ongoing study to find the best possible model for the prediction of shock-wave/boundary-layer flow interactions.

Models and Computations

In the present work, four turbulence models were chosen for comparison; namely, the standard $k - \epsilon$ [1], the two-scale $k - \epsilon$ [2], the RNG $k - \epsilon$ [3] and the realizable $k - \epsilon$ [4] models. All models tested were high-Reynolds number versions and the compressible wall functions proposed by Huang and Coakley [5] were used to connect the first grid point to the wall. The first grid line is adjusted to ensure that it is in the fully turbulent region (y^+ is between 30 and 50).

The problem involves a 2-D compression corner flow (description of the test problem can be found in Settles and Dodson [6].), which was proposed in the 1980-1981 AFOSR-HTTM-Stanford Conference on complex turbulent flows as a possible candidate for testing turbulence models in predicting flows with shock-wave/boundary-layer interactions. The experiment deals with a 2-D ramp placed on the bottom wall of a wind tunnel to create shock wave that interferes with the wall boundary layer. The Mach number was 2.8 to 2.9, the incoming boundary layer momentum thickness was about 0.13 cm and the free-stream unit Reynolds number was $6.3 \times 10^7/m$.

The Navier-Stokes code developed by Huang and Coakley [7] was used in this study. Calculations were performed in two stages. The first stage involves the solution of a flow over a flat plate to obtain the mean and the turbulent property profiles for the boundary layer corresponding to the test conditions before the interaction. The matching is based on the boundary layer displacement thickness and as can be seen later, all models produce mean velocity profiels that agree very well with measurements at the first station. The second stage involves calculations in the interaction zone (s varies from -15 cm to 15 cm). The corner is located at $s = 0$. The inlet conditions were taken from the solution established in the first stage. Two sets of grid mesh (120×80 and 80×50) were tested in the 24^o case (case D). The results were found to be grid independent. The results reported in the next section were obtained using the finer mesh.

Results and Discussion

Figures. 1 and 2 show the predictions of the pressure coefficient, $C_p = p_w/p_\infty$, and the skin friction coefficient, $C_f = 2\tau_w/\rho_\infty U_\infty^2$, for the 8° case. Computations based on all the models give good predictions of the pressure coefficients, figure 1. The predicted skin friction coefficients, figure 2, compare fairly well with data, considering the reported measurement uncertainty is as high as 15%. The velocity profile comparison is shown in figure 3. The predicted results were almost identical and agree well with experimental data.

Predictions of the pressure and the skin friction coefficients for the 16° case are shown in figures 4 and 5, respectively. The pressure coefficients were predicted well by all models, but one starts to see differences in model performance when comparing the skin friction coefficients in the recovery region. As can be seen from the figure, both the $k-\epsilon$ and two-scale models predicted overshoot of the skin friction coefficients in the recovery region, while the skin-friction coefficients predicted by the RNG and the realizable models are in better agreement with experimental data. Figure 6 shows the comparison of the velocity profiles. Differences in model predictions can only be seen near the compression corner. The results calculated by using the RNG and the realizable models show that the flow very close to the wall is slightly more retarded than the prediction made by using the two other models. While the differences in model performance can be observed in the near wall region, all models predicted the flow behavior very well away from the surface.

Model predictions begin to show large differences in the 20° case where the flow has separated. Figures 7 and 8 show comparisons of the skin-friction and the pressure coefficients with experiment. As can be seen from figure 8, both the RNG and the realizable models show a larger size of flow separation than the experimental data. While the standard $k-\epsilon$ and the two-scale models predict a flow separation in better agreement with data, they slightly over-predict the skin friction coefficients in the recovery region. The larger sizes of the flow separation predicted by the RNG and the realizable models were also reflected in the comparison of the velocity profiles. Figure 9 shows that the velocity profiles predicted by the standard $k - \epsilon$ and the two-scale models are better matched with the experimental data and the other two models display a larger departure from the experimental data in the near wall region.

At 24°, the flow is separated and the comparison of the pressure and the skin friction coefficients clearly shows that the RNG and the realizable models over-predicted the size of flow separation and the standard $k - \epsilon$ and the two scale models under-predicted it, as can be seen from figures 10 and 11. The prediction of the skin friction coefficients in the recovery region shows mixed results, but in general all models show a good rate of recovery of the skin friction coefficients, $\partial C_f/\partial s$. The differences in the results are largely caused by the models' deficiency in predicting flow separation. The deficiency manifests itself when the velocity profiles are compared. As can be seen from figure 12, the RNG and the realizable models show excess retardation of the velocity profiles in the near wall region while the standard $k - \epsilon$ and two-scale models show results in better agreement with experimental data.

Conclusions

While there were some evidence to show that the newer, modified $k - \epsilon$ models were capable of predicting separated flows, our experience in this study has shown otherwise. Overall, all models perform well in flows without separation and the differences in the model predictions are small. Differences arise when the flow is separated. We have found that the RNG and the realizable models tend to over-predict the flow separation and the standard $k - \epsilon$ and the two-scale model tend to under-predict it. The success of a model in predicting velocity profiles and the skin-friction and pressure coefficients is strongly affected by the model's ability in predicting flow separation. Hence, the capability of the model in predicting incipient flow separation becomes an important factor in a successful calculation of shock-wave/boundary-layer flow interactions.

References

1. Launder, B. E. and Spalding, D. B., Comp. Methods in Applied Mech. and Eng., 3, 1974.
2. Liou, W. W. and Shih, T.-H., NASA TM 106072, 1993.
3. Yakhot, V., Orszag, S. A., Thangam, S., Gatski, T. B. and Speziale, C. G., Phys. Fluids A, 4, 1992.
4. Zhu, J. and Shih, T. H., NASA TM 106154, 1993.
5. Huang, P. G. and Coakley, T. J., AIAA-92-0547, 1992.
6. Settles, G. S. and Dodson, L. J., NASA CR 177577, 1991.
7. Huang, P. G. and Coakley, T. J., 2nd Int. Sym. on Engr. Turbulence Modelling and Measurements, Florence, Italy, 1993.

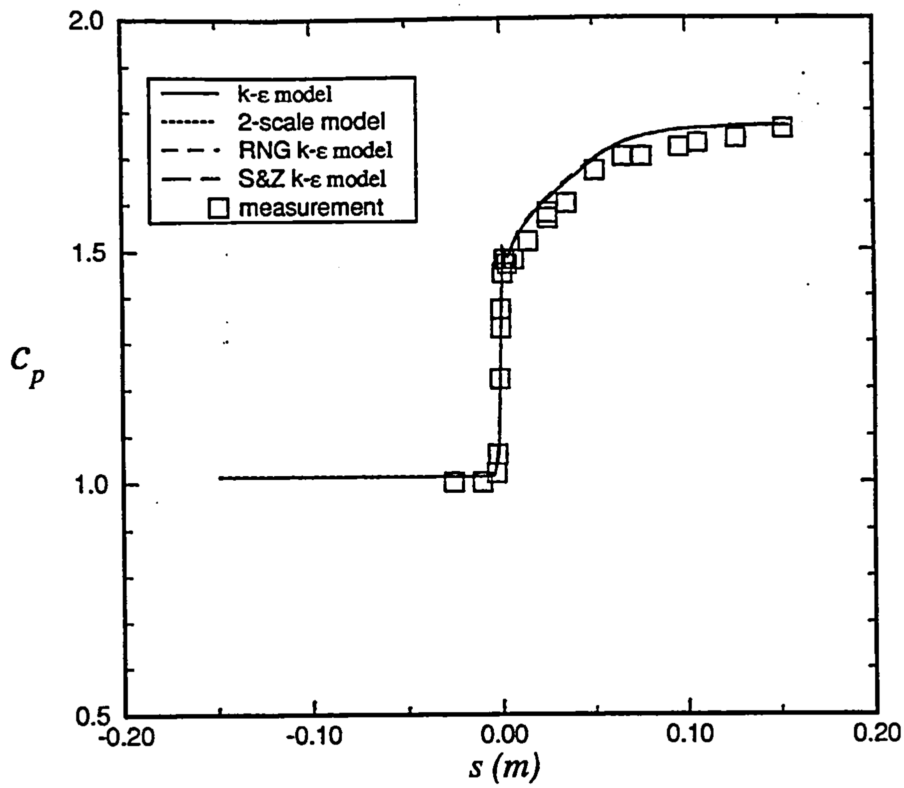

Figure 1. Wall pressure coefficients for 8° ramp.

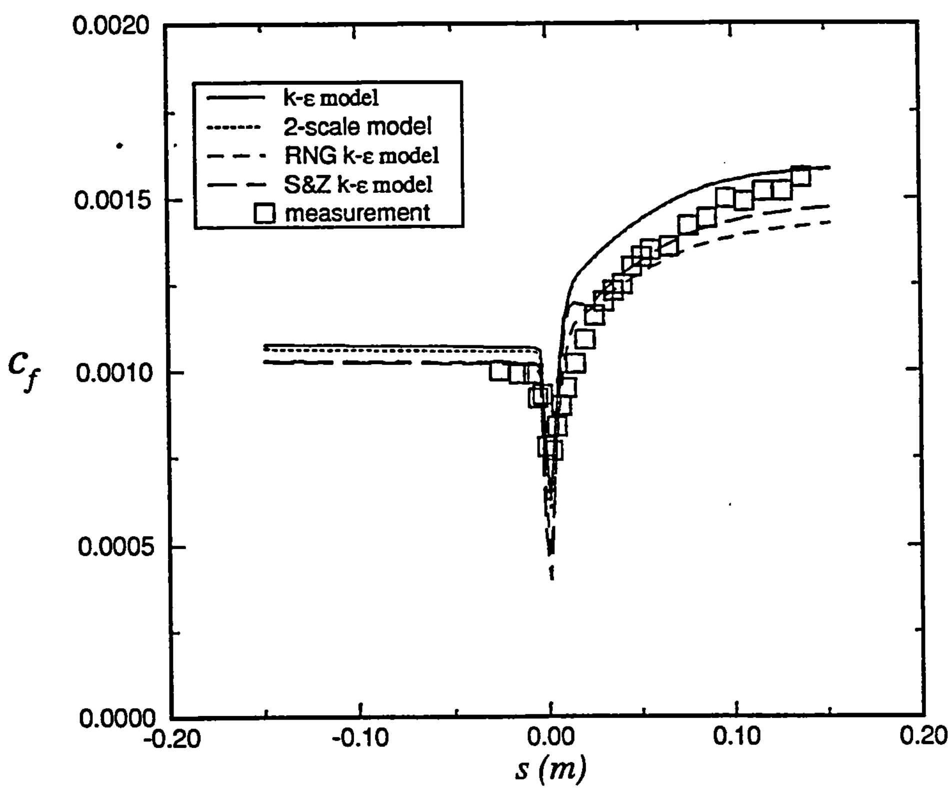

Figure 2. Skin-friction coefficients for 8° ramp.

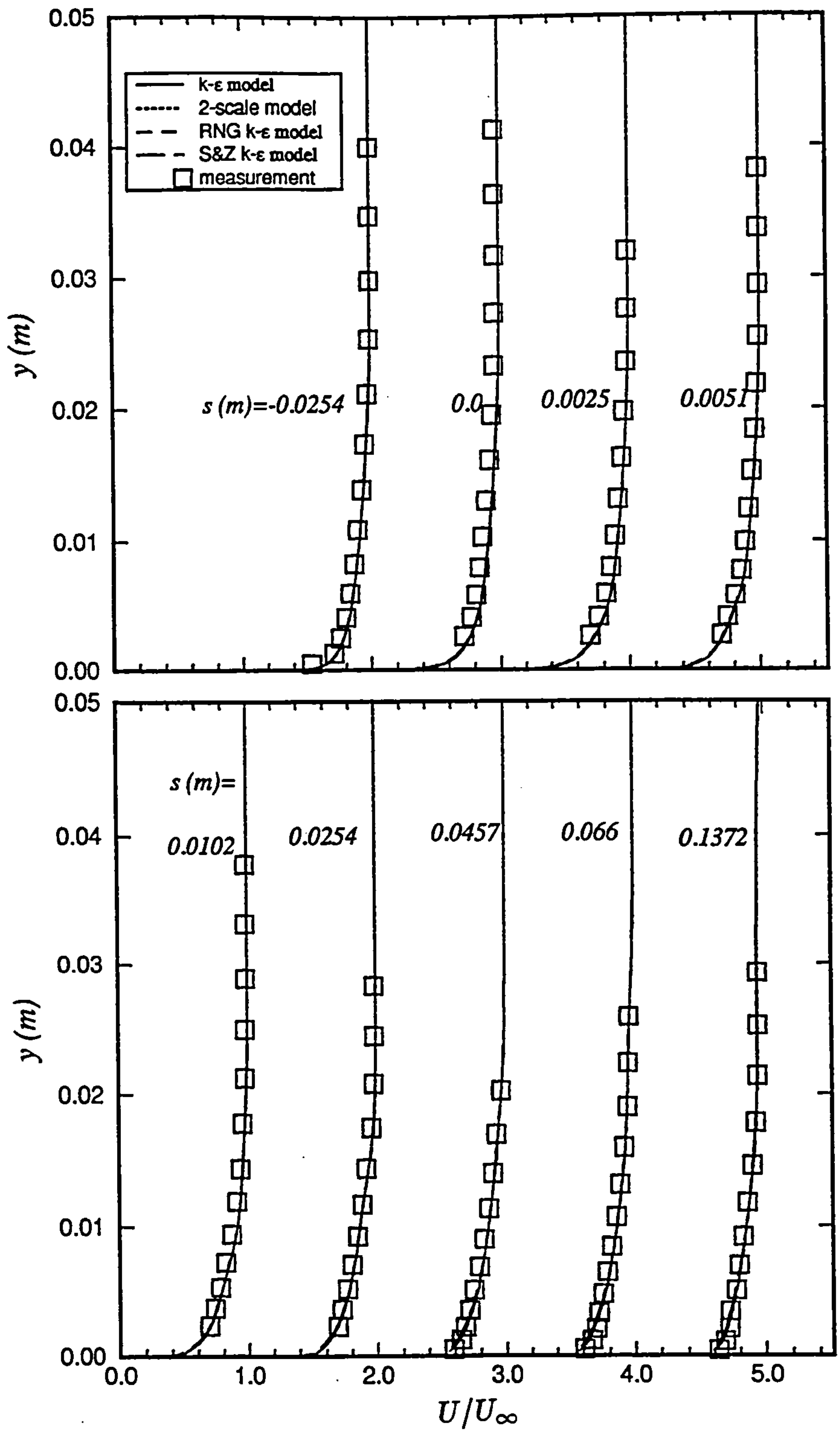

Figure 3. Mean velocity profiles for 8° ramp.

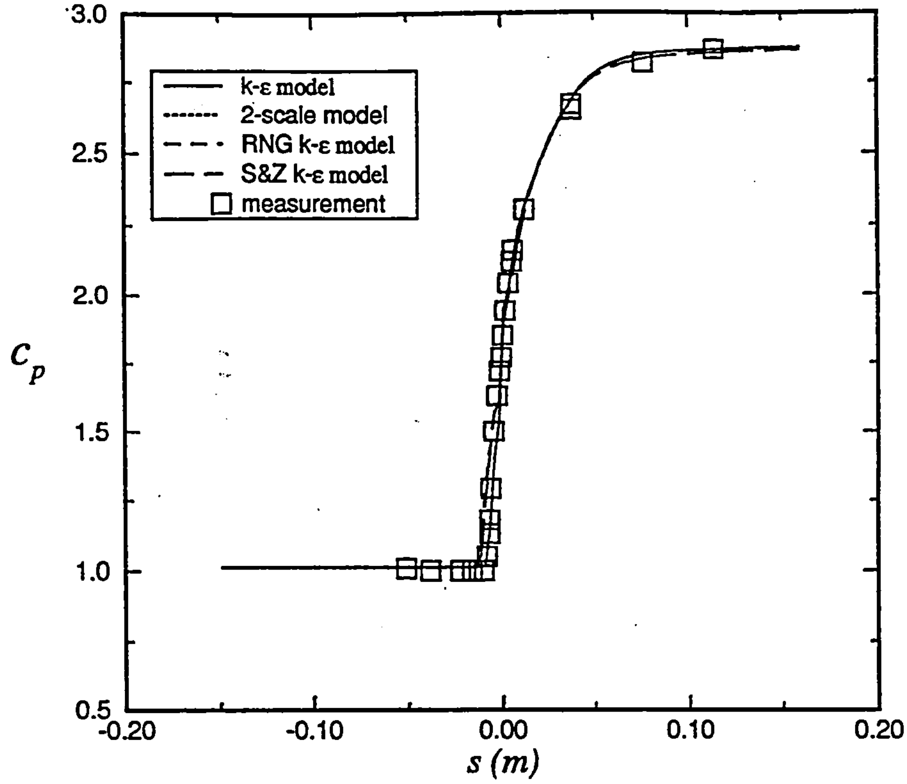

Figure 4. Wall pressure coefficients for 16° ramp.

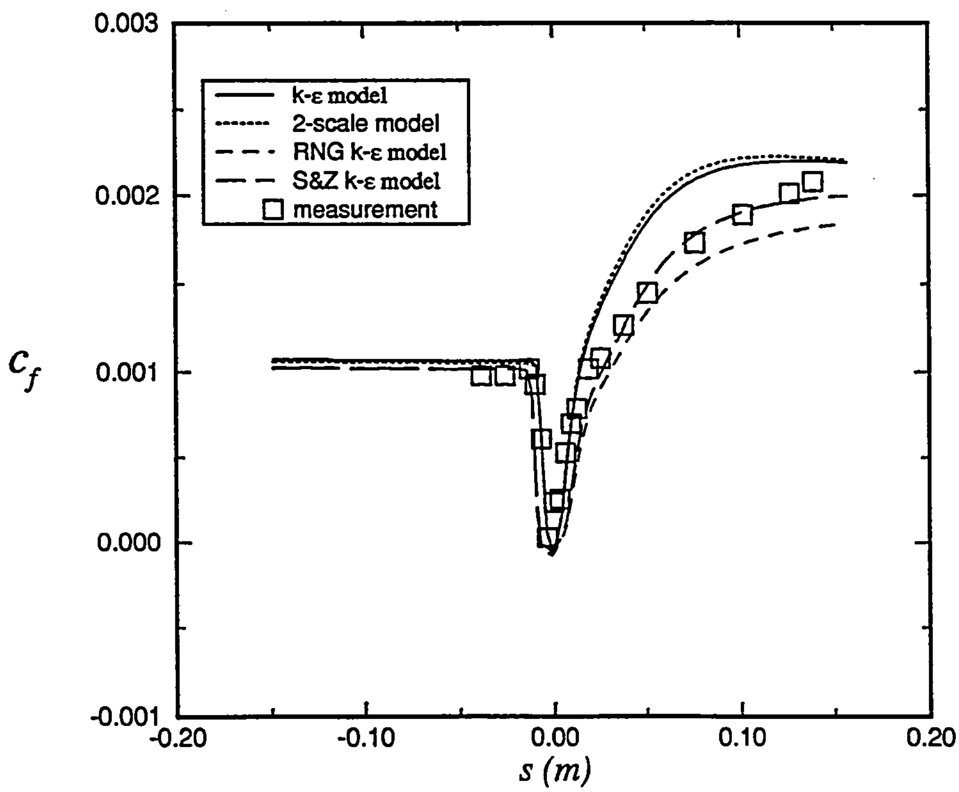

Figure 5. Skin-friction coefficients for 16° ramp.

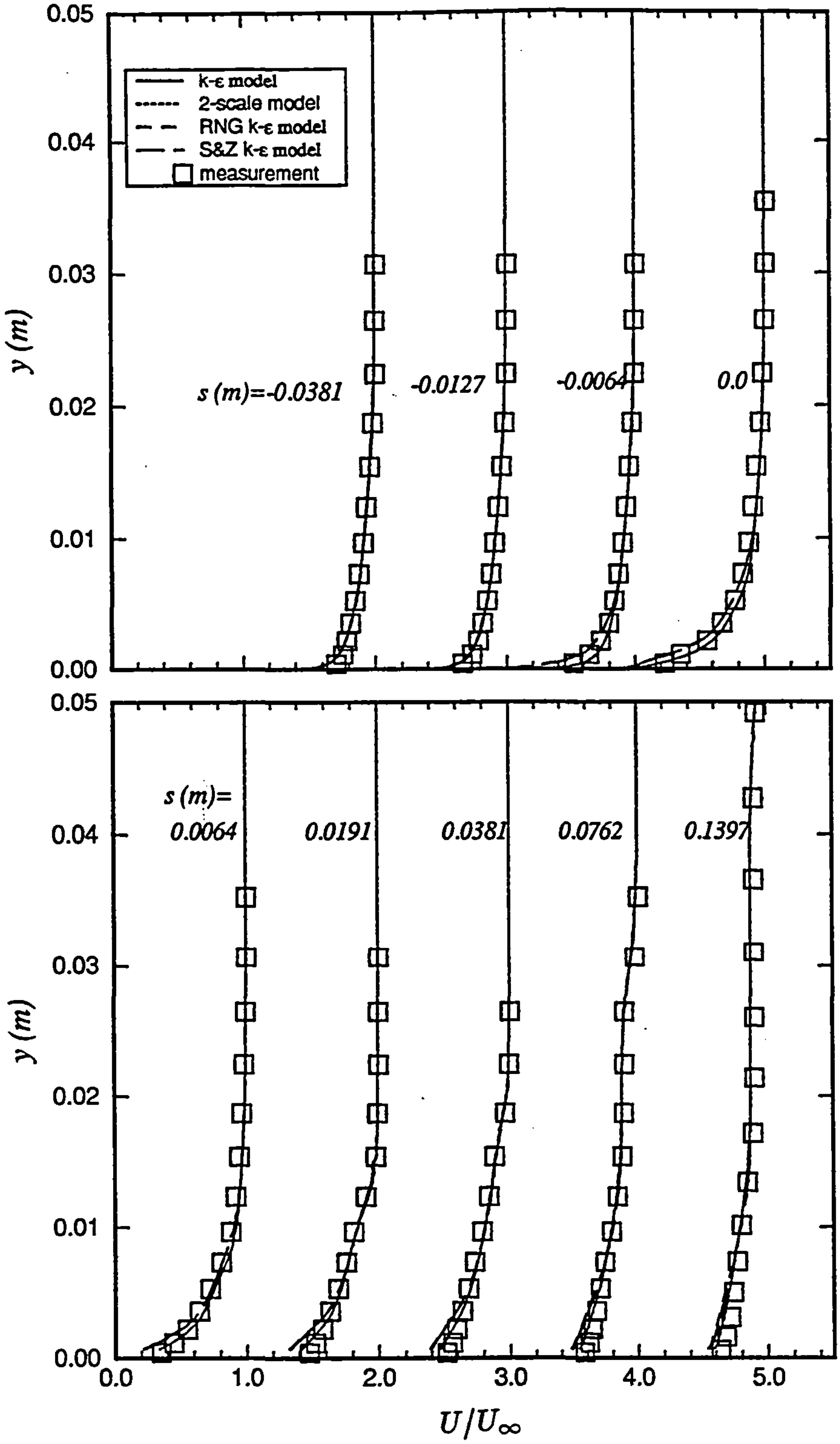

Figure 6. Mean velocity profiles for 16° ramp.

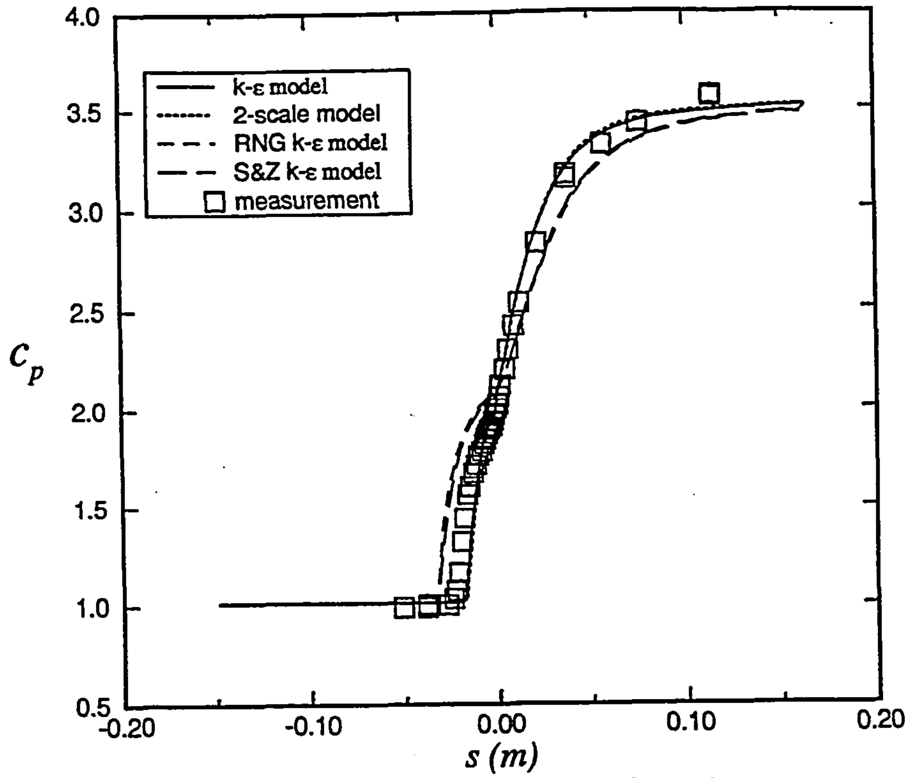

Figure 7. Wall pressure coefficients for 20° ramp.

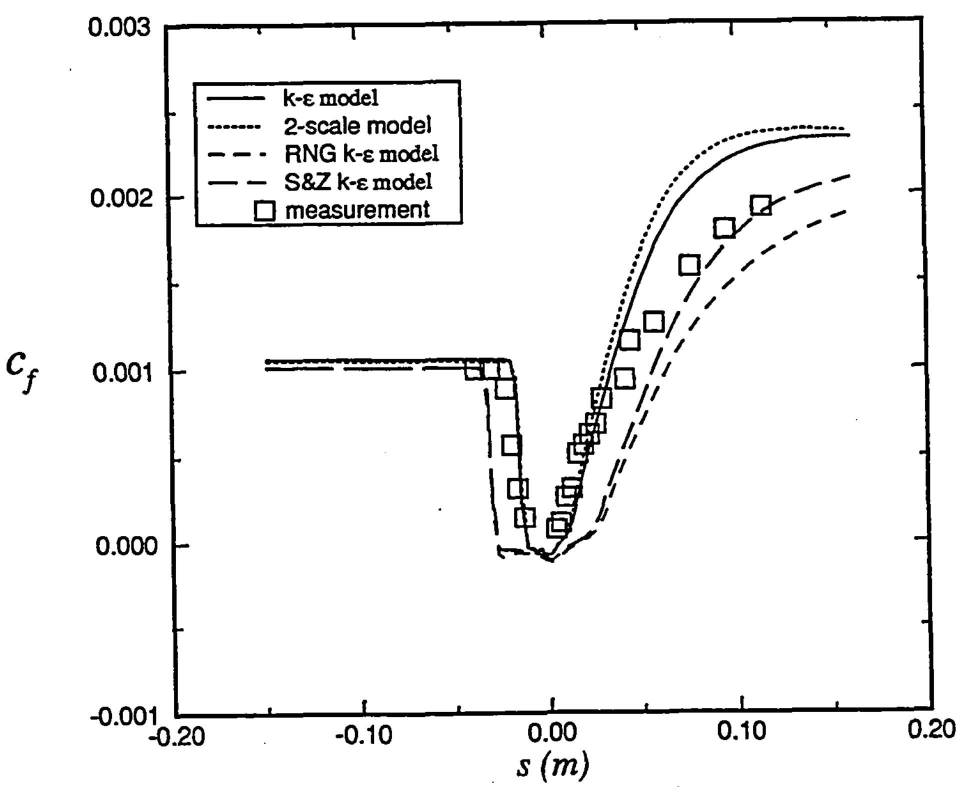

Figure 8. Skin-friction coefficients for 20° ramp.

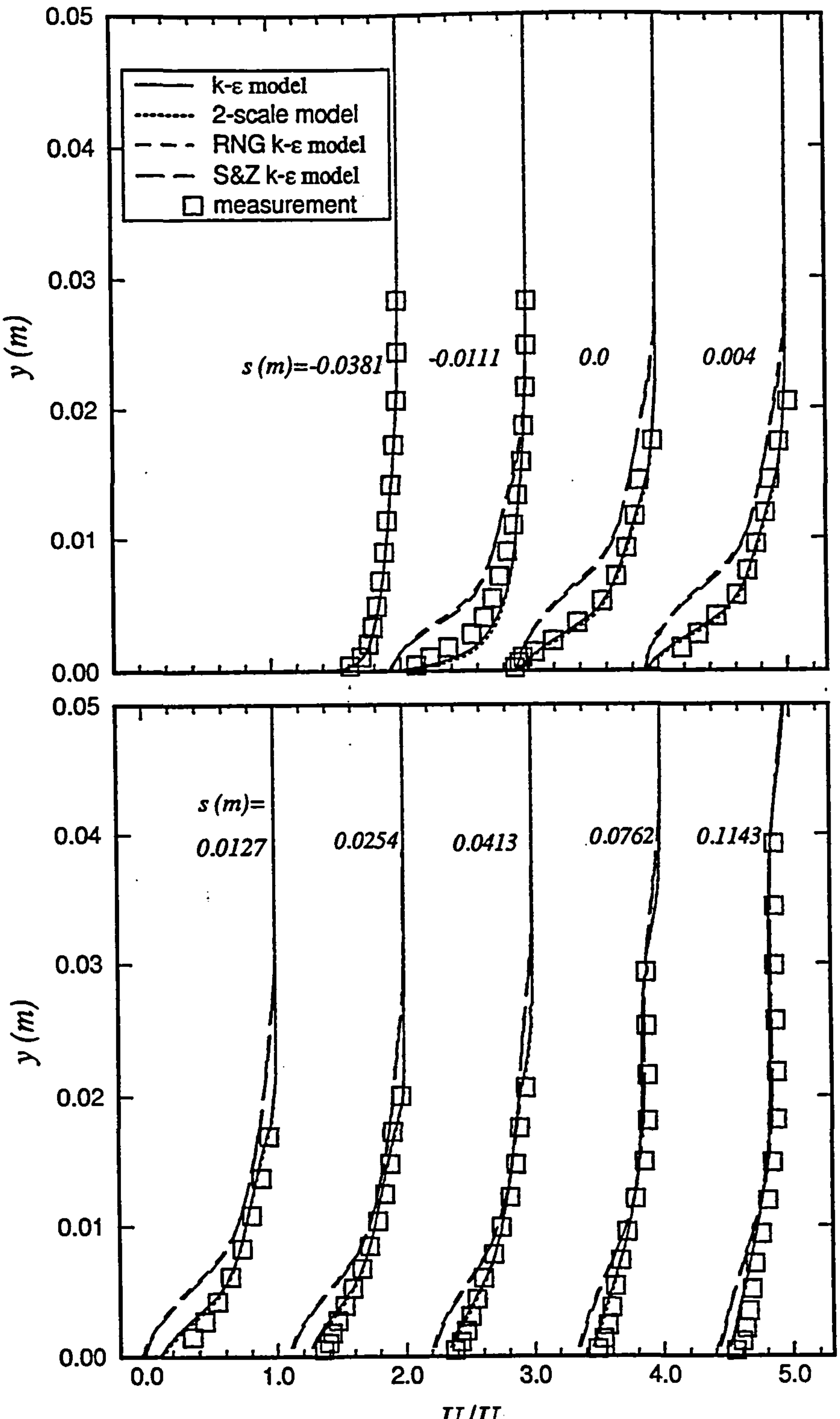

Figure 9. Mean velocity profiles for 20° ramp.

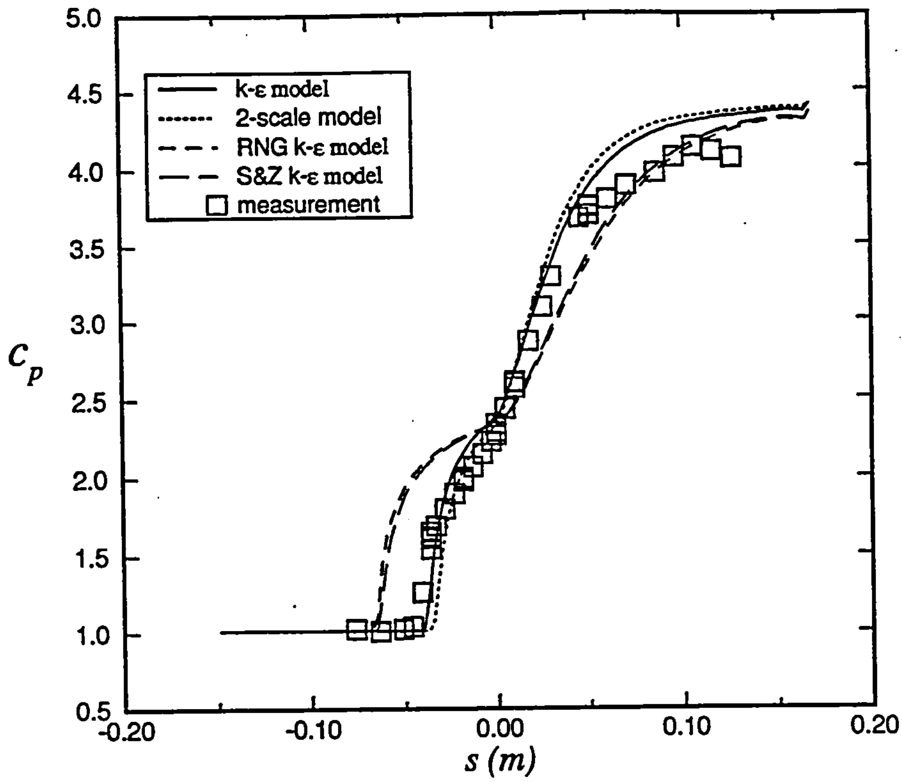

Figure 10. Wall pressure coefficients for 24° ramp.

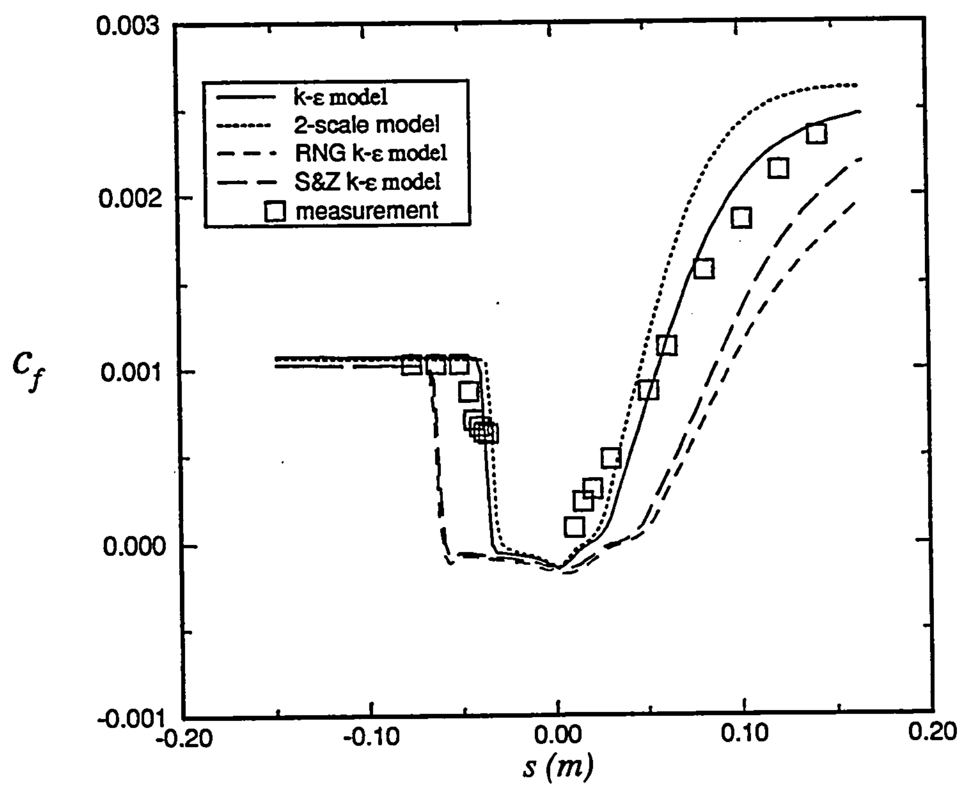

Figure 11. Skin-friction coefficients for 24° ramp.

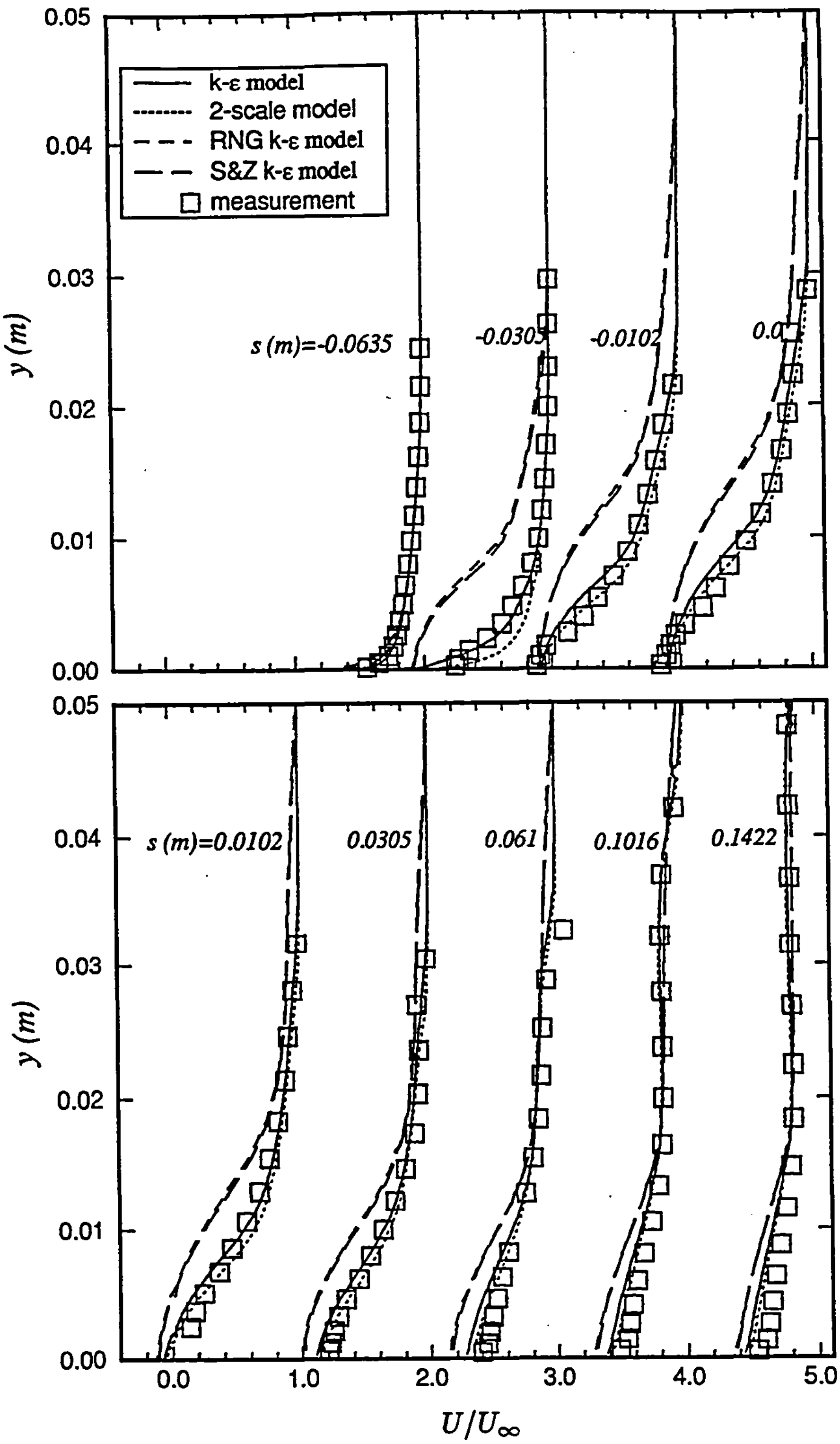

Figure 12. Mean velocity profiles for 24° ramp.

REPORT DOCUMENTATION PAGE

Form Approved
OMB No. 0704-0188

1. AGENCY USE ONLY (*Leave blank*)	2. REPORT DATE	3. REPORT TYPE AND DATES COVERED
	August 1994	Technical Memorandum

4. TITLE AND SUBTITLE

Numerical Calculations of Shock-Wave/Boundary-Layer Flow Interactions

5. FUNDING NUMBERS

WU–505–90–5K

6. AUTHOR(S)

P.G. Huang and W.W. Liou

7. PERFORMING ORGANIZATION NAME(S) AND ADDRESS(ES)

National Aeronautics and Space Administration
Lewis Research Center
Cleveland, Ohio 44135–3191

8. PERFORMING ORGANIZATION REPORT NUMBER

E–9049

9. SPONSORING/MONITORING AGENCY NAME(S) AND ADDRESS(ES)

National Aeronautics and Space Administration
Washington, D.C. 20546–0001

10. SPONSORING/MONITORING AGENCY REPORT NUMBER

NASA TM–106694
ICOMP–94–16
CMOTT–94–4

11. SUPPLEMENTARY NOTES

Prepared for the First International Conference on Flow Interactions sponsored by Hong Kong University, Hong Kong, September 5–9, 1994. P.G. Huang, Eloret Institute, Palo Alto, California, and W.W. Liou, Institute for Computational Mechanics in Propulsion and Center for Modeling of Turbulence and Transition, NASA Lewis Research Center (work funded by NASA Cooperative Agreement NCC3–233). ICOMP Program Director, Louis A. Povinelli, organization code 2600, (216) 433–5818.

12a. DISTRIBUTION/AVAILABILITY STATEMENT	12b. DISTRIBUTION CODE
Unclassified - Unlimited Subject Category 34	

13. ABSTRACT ***(Maximum 200 words)***

The paper presents results of calculations for 2-D supersonic turbulent compression corner flows. The results seem to indicate that the newer, improved κ - ϵ models offer limited advantages over the standard κ - ϵ model in predicting the shock-wave/boundary-layer flows in the 2-D compression corner over a wide range of corner angles and flow conditions.

14. SUBJECT TERMS	15. NUMBER OF PAGES
Shock waves; Boundary layer interactions	14
	16. PRICE CODE
	A03

17. SECURITY CLASSIFICATION OF REPORT	18. SECURITY CLASSIFICATION OF THIS PAGE	19. SECURITY CLASSIFICATION OF ABSTRACT	20. LIMITATION OF ABSTRACT
Unclassified	Unclassified	Unclassified	

NSN 7540-01-280-5500

Standard Form 298 (Rev. 2-89)
Prescribed by ANSI Std. Z39-18
298-102

National Aeronautics and
Space Administration
Lewis Research Center
Cleveland, OH 44135-3191
ICOMP OAI